2018 European Control Conference (ECC)
June 12-15, 2018. Limassol, Cyprus

Robust Loop-Shaping Control Design and Implementation for an Automatic Neuro-Developmental-Treatment Device

Fu-Cheng Wang*, Yu-You Lin, and Chung-Huang Yu

Abstract—**This paper applies robust control to an automated device that are developed to assist neuro-developmental treatment (NDT) rehabilitation. NDT training is an effective rehabilitation for stroke patients but labor-intensive for therapists. Hence, patients usually do not have sufficient training because of the shortage of therapist assistance. The purpose of this paper is to develop an automated device that can help NDT training and reduce therapists' workloads. We first record the therapist's actions and the test subject's motions during NDT training. Then we develop an automatic NDT trainer that can repeat the therapist's intervention by motor control systems. We apply robust loop-shaping control to cope with the system variation during the training. Last, we conduct experiments and discuss the effectiveness of the designed NDT trainer by two specified performance indexes.**

I. INTRODUCTION

Stroke is a common disease with a high mortality rate. Patients, even luckily surviving the accidents, still needs long-term treatment and rehabilitation training [1, 2]. The expenditure for stroke treatments imposes a heavy load on society and on individuals; e.g. in USA each stroke patient spends about US$54,000 on rehabilitation treatments [3]. The purpose of rehabilitation is to allow the patients to recover their capacity for independent living, particularly walking by themselves. Several lower-limb rehabilitation robots have been developed to restore mobility of the affected limbs [4]. For example, Colombo et al. [5] designed a driven gait orthosis (DGO) to guide a patient's legs on a moving treadmill. They analyzed gait parameters and derived optimal training programs that can be reproduced by the DGO. Schmidt et al. [6] proposed the HapticWalker with six degrees of freedom (DOF) force sensors for wheelchair-mobilized patients. Patton et al. [7] designed a robotic device (KineAssist) for gait and balance training. The device provided partial body weight support (BWS) and postural control on the torso, so that the patient's legs were accessible to the therapists' manipulation when walking. Schmitt et al. [8] presented an active functional device (MotionMaker) that had two orthoses with motors and sensors. The device can manage real-time electrical stimulation that controls leg movements according to the desired positions, speeds, and torques. Belforte et al. [9] designed an active gait orthosis with electro-pneumatic circuits to assist locomotion in paraplegic subjects.

Fu-Cheng Wang is with the Department of Mechanical Engineering, National Taiwan University, Taipei, Taiwan. (phone: +886233662680; fax: +886223731755; e-mail: fcw@ntu.edu.tw).

Yu-You Lin is with the Department of Mechanical Engineering, National Taiwan University, Taipei, Taiwan. (e-mail: r04522815@ntu.edu.tw).

Chung-Huang Yu is with the Department of Physical Therapy & Assistive Technology, National Yang-Ming University, New Taipei City, Taiwan. (e-mail: chyu@ym.edu.tw).

Compared with these devices that guide the patients to follow preset preferred gaits, neuro-developmental treatment (NDT) training is a way to let the patients have the feeling of walking with minimal guidance and facilitation. During the training, the patients intentionally drive their center of gravity (COG) forward and balance themselves using striding steps and feeling the COG conversion [10]. NDT training is effective for stroke survivors but very labor intensive for therapists [10-12]. Therefore, we design a NDT trainer and apply control techniques to help relieve the therapists' workloads and to assist the patients' rehabilitation. First, we record the experimental data during clinical NDT training and build an expert database. Second, we construct a mechanism and apply robust loop-shaping control to imitate the therapists' actions based on the expert database. Last, we integrate the system and conduct experiments on test subjects. The results indicate that the designed NDT trainer and controller can effectively repeat the therapists' actions during the training and help rehabilitation processes.

This paper is arranged as follows: Section II introduces the proposed NDT trainer. Section III shows the clinical data during NDT training and builds an expert database. Section 4 constructs a control system and designs a robust loop-shaping controller to imitate the therapists' actions during NDT training. Section 5 applies the trainer for experimental verification. We define two performance indexes to evaluate the effectiveness of the automatic training device. Finally, we draw conclusions in Section 6.

II. SYSTEM DESCRIPTION

The designed NDT trainer is shown in Fig. 1(a), where the test subject is connected to the BWS. We attach two ropes to the subject's anterior-superior-iliac spine (ASIS) to stimulate the gaits. The subjects can be guided by therapists or by the automatic NDT trainer through the ropes. The system structure is shown in Fig. 1(b). We apply a motion capture system VZ4000 [13] to record the motions of the test subjects during the NDT training. The VZ4000 can detect a displacement of 0.015 mm at a distance of 1.2 m with a sampling rate of 100Hz and a root mean square error of 0.5mm. Two VZ 4000 trackers are used to detect the LED markers attached to the test subjects for gait measurements. We set the LED markers according to the Helen Hayes Marker Set [14]: four on the waist, two on the thighs, two on the knees, two on the shanks, two on the ankles, two on the toes, and two on the heels. The therapists conduct NDT training by pulling the ropes to motivate the patient's gaits, so that we implement load cells [15] to record the pulling forces. These data are transmitted to an embedded National

Instrument (NI) myRIO microcontroller [16]. We will analyze the therapists' actions and design an automatic device to repeat them for NDT training. The specifications of the system components are illustrated in Table I.

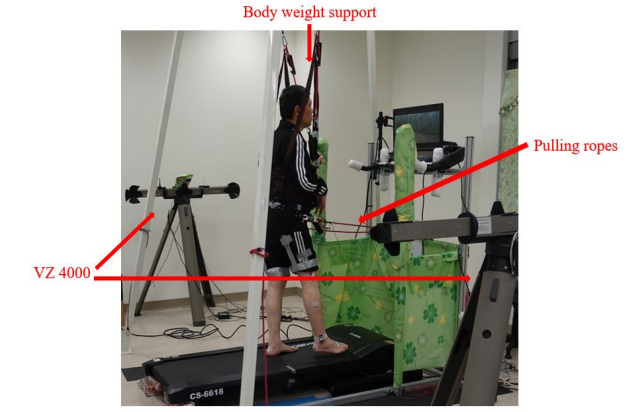

(a) The experimental layout.

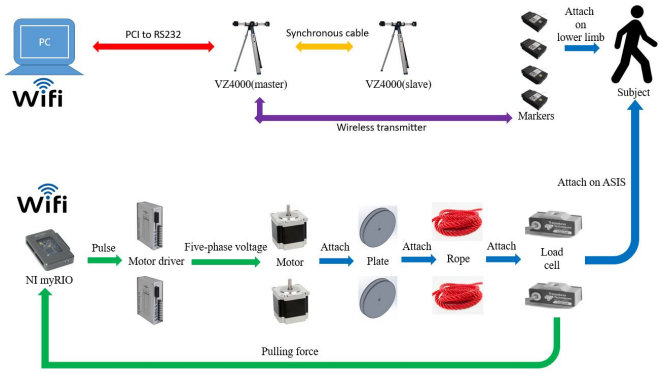

(b) The system structure.

Fig. 1 The proposed automatic NDT trainer.

TABLE I. SYSTEM SPECIFICATIONS

VZ 4000	
Distance range	1.2 m
Sensor resolution	0.015 mm
Accuracy	0.5 mm RMS
Load cell (DPM-3)	
Read rate	60 Hz
Input voltage	85-264 Vac or 90-300 Vdc
Output voltage	-10 to +10V
Output current	0~20mA
Sensor resolution	±0.02% of full scale analog output
Maximum force	50 lb
NI myRIO	
# Analog input	10
# Analog output	6
# Digital I/O	40
CPU	Xilinx FPGA & ARM Cortex™-A9
Clock rate	40MHz
Stepper motor (MPK-569-2.8A)	
Phase	5 phase
Step angle	0.72 °/step
Voltage	1.75 V
Current	2.8 A/phase
Resistance	0.62 ±10% Ω /phase
Inductance	1.1 ±20% mH/phase
Holding torque	16kgf cm

III. MOTION ANALYSES

We invite the therapists to conduct NDT training and observe their actions on the test subjects. The therapists guide the subject's movements using the ropes that are attached to the subject's ASIS. We measure and analyze the therapists' forces and the subjects' motions to derive patterns of the therapists' actions.

A complete gait cycle is defined as the period from the initial contact of the stance leg with the ground to the next initial contact of the same leg, as shown in Fig. 2 [17]. A gait cycle is conventionally divided into stance and swing phases, with durations of about 60% and 40%, respectively. The stance phase consists of the following periods: (A) initial contact, (B) loading response (foot flat), (C) mid-stance, (D) terminal stance (heel off), and (E) pre-swing (toe off). The swing phase is composed of (F) initial & mid-swing, and (G) terminal swing. The double support periods (A and E), which occur twice during a complete gait cycle, are defined as the duration from when the heel first contacts the ground to when the toes of the other foot take off from the ground.

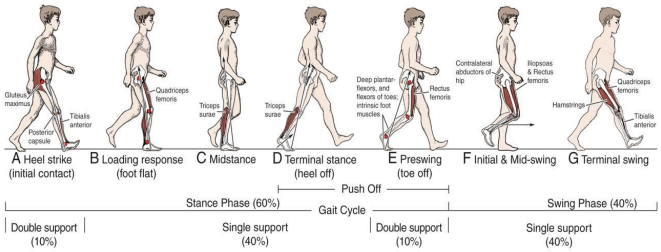

Fig. 2 The gait cycle [17].

We invite several subjects to participate the experiments. These testing subjects have signed informed consent forms approved by Human Subject Research Ethics Committee of Institutional Review Board (IRB). We record the position and load-cell data. The load-cell data is divided into gait cycles, when the therapist guides the subject's gait by pulling the ropes. For example, the forces applied on the left ASIS and the heights of the right heel of subject 1 are shown in Fig. 3, where the x-axis represents the percentage of each gait cycle. Note that the therapist applies forces on the opposite ASIS at about the time when the heel struck the ground ((A), (D) and (G) periods in Fig. 2). Therefore, we will design the NDT gait trainer based on these patterns.

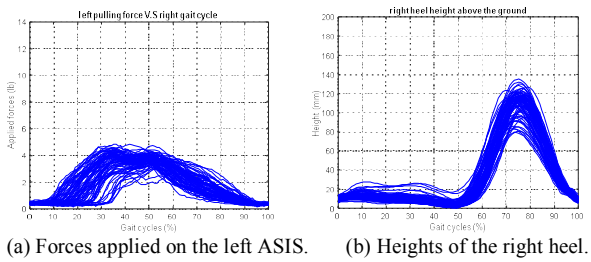

(a) Forces applied on the left ASIS. (b) Heights of the right heel.

Fig. 3 Intervention analyses.

Fig. 4(a) shows the standard therapists' pulling forces, which are periodic. Therefore, we take Fast Fourier Transform (FFT) and show the frequency responses in Fig. 4(b), where the left and right sides have the same dominant frequency. Because the force profiles are similar to sinusoidal waves, we can reconstruct the forces profiles as follows:

$$(F_{\max} - F_{\min}) \times \sin(2\pi ft) + F_{\min} \quad (1)$$

where $F_{\max}$ and $F_{\min}$ represent the average maximum and minimum, respectively, of the applied forces. f is the dominant frequency. Therefore, we can build a control system to track the force commands of (1).

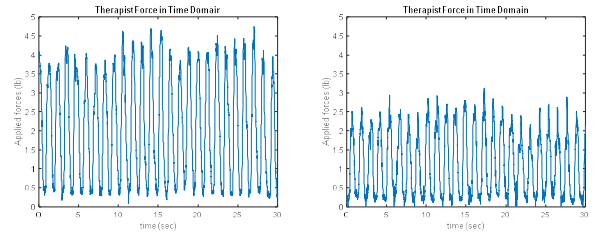

(Left ASIS) (Right ASIS)

(a) Time responses.

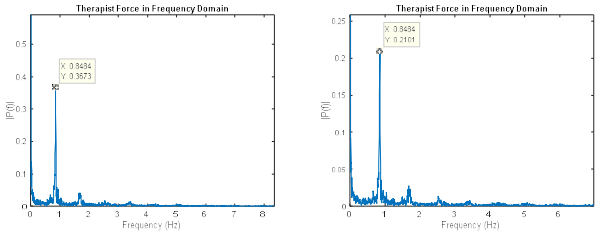

(Left ASIS) (Right ASIS)

(b) FFT of the applied forces.

Fig. 4 Analyses of the applied forces.

IV. Identification and Control of the Motor System

This section developed a motor control system to repeats the therapists' actions, as shown in Fig. 5. The system's transfer functions are derived by experiments, in which the load cells are connected to the ground. We can regard human behavior as model variation and disturbances, and apply robust control techniques to cope with these model uncertainties during automatic NDT training.

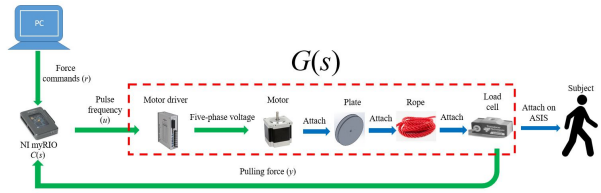

Fig. 5. The motor control system.

A. System identification

Stepper motors [18] are used to drive the ropes, as shown in Fig. 5. The input (u) is the frequency of pulse signals, while the output (y) represents the pulling forces. We apply the closed-loop identification method [19] to derive the motor models. First, we use a swept sinusoidal input command (r) with a magnitude of 1.5~6 lb at the frequency range of 0.1~3 Hz, as shown in Fig. 4. Then we measure the pulse frequency (u) and output force (y). Last, we apply the numerical subspace state space system identification (N4SID) method [20] to derive the transfer functions of the motor system. Considering the system variations, we repeat the experiment ten times and obtain the following transfer functions:

$$G_i(s) = T^i_{u\to y}, \; i = 1,\ 2,\ \ldots,\ 10 \quad (2)$$

where G_i represents the model derived from the i-th experiment. We note the model variation of (2), which might cause stability and performance problems during operation. Therefore, robust control techniques are applied to improve system stability and performance.

We can regard the systems as a nominal model G_0 with uncertainties. Suppose G_0 has the following left coprime factorization (LCF) [21]:

$$G_0 = \tilde{M}^{-1}\tilde{N},$$

in which $\tilde{M}, \tilde{N} \in RH_\infty$ and $\tilde{M}\tilde{M}^* + \tilde{N}\tilde{N}^* = I$. A perturbed plant G_Δ can be represented as follows:

$$G_\Delta = \left(\tilde{M} + \Delta_{\tilde{M}}\right)^{-1}\left(\tilde{N} + \Delta_{\tilde{N}}\right),$$

where $\Delta_{\tilde{M}}, \Delta_{\tilde{N}} \in RH_\infty$. Because the coprime factorization of a system is not unique, we can define the gap between the nominal plant G_0 and the perturbed plant G_Δ as [22]:

The smallest value of $\left\|\begin{bmatrix}\Delta_{\tilde{M}} & \Delta_{\tilde{N}}\end{bmatrix}\right\|_\infty \le \varepsilon$ *, which perturbs* G_0 *into* G_Δ*, is called the gap between* G_0 *into* G_Δ *and is denoted as* $\delta(G_0 \quad G_\Delta)$.

Therefore, we select the nominal plant G_0 from the derived ten transfer functions that minimizes the maximum gaps between G_0 and G_i, as in the following:

$$G_0 = \arg\min_{G_0} \max_{G_i} \delta(G_0,\ G_i),\ \forall G_i$$
$$= \frac{-21.39s + 339.4}{s^2 + 39.09s + 64.89}$$

which gives a system gap of $\delta(G_0, G_i) \le 0.019427,\ \forall i$. The gap can be regarded as the maximum system variations due to system uncertainties and operating conditions.

B. Robust Loop-Shaping control design

A closed-loop system with a perturbed plant G_Δ and a controller K can be expressed as Fig. 6(a), and rearranged as Fig. 6(b). From the Small Gain Theorem [23], the closed-loop system is internally stable for all perturbations with $\left\|\begin{bmatrix}\Delta_{\tilde{M}} & \Delta_{\tilde{N}}\end{bmatrix}\right\|_\infty \le \varepsilon$ if and only if

$$\left\|\begin{bmatrix}K\\ I\end{bmatrix}(I - G_0K)^{-1}\tilde{M}^{-1}\right\|_\infty = \left\|\begin{bmatrix}K\\ I\end{bmatrix}(I - G_0K)^{-1}\tilde{M}^{-1}\begin{bmatrix}I & G_0\end{bmatrix}\right\|_\infty < \frac{1}{\varepsilon}$$

Hence, we can further define the system's stability margin $b(G_0, K)$ as:

$$b(G_0,K) = \left\| \begin{bmatrix} K \\ I \end{bmatrix} (I - G_0 K)^{-1} \tilde{M}^{-1} \begin{bmatrix} I & G_0 \end{bmatrix} \right\|_\infty^{-1} \quad (7)$$

The system is then internally stable for all uncertainties Δ with $\|\Delta\|_\infty = \left\| \begin{bmatrix} \Delta_{\tilde{M}} & \Delta_{\tilde{N}} \end{bmatrix} \right\|_\infty \le \varepsilon$, if and only if $b(G_0, K) > \varepsilon$. Therefore, the goal of robust control is to design a controller K for the nominal plant G_0 such that the stability margin $b(G_0, K)$ is greater than the system gaps $\delta(G_0, G_i), \forall G_i$.

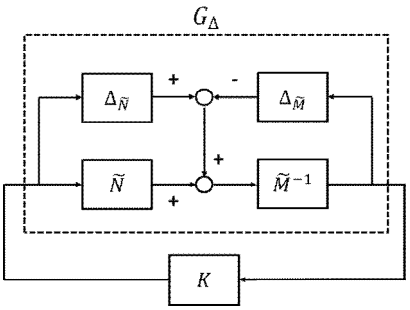

(a) The closed-loop system.

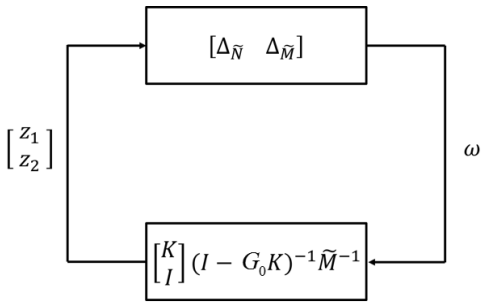

(b) Small-Gain Theorem block.

Fig. 6 Stability analysis.

We apply H_∞ loop-shaping techniques [24] to improve system performance. The principles of loop shaping are: (1) increasing system gains at the low-frequency ranges for disturbance rejection; (2) decreasing system gains at the high-frequency range for attenuating noises; and (3) limiting the slope of the magnitude plots around cross-over frequencies less steep than -40 dB/decade for stability consideration. We iteratively adjust the weighting functions and verify the system performance by experiments. Finally, we select the following weighting function:

$$W = \frac{4s + 0.8}{0.1225s^2 + 0.7s + 1}$$

and design the corresponding robust controller as follows:

$$K_\infty = \frac{3.746s^2 + 171.8s + 1131}{s^2 + 84.06s + 5588}$$

which gives a stability margins of $b(WG_0, K_\infty) = 0.2579$, which is much greater than the system gaps (0.019427) and can guarantee the system stability during operations. The loop-shaping design is illustrated in Fig. 7(a).

C. *Pre-compensator design*

We can note the phase lag in Fig. 7(a), which might result in unsynchronized responses during the training. Therefore, we further design a phase-lead pre-compensator, as shown in Fig. 7(b), to improve the tracking performance. The phase lead pre-compensator was designed as:

$$C_{pre}(s) = 0.737 \frac{s/6.5 + 1}{s/40 + 1}$$

We test the motor's tracking ability and show the simulation and experiment results in Fig. 7(c). First, the phase-lag is successfully eliminated by the phase-lead pre-compensator. Second, the root mean square errors of the simulation and experiments are 0.0472lb and 0.4817lb, respectively. That is, the designed motor control mechanism can track the desired force patterns.

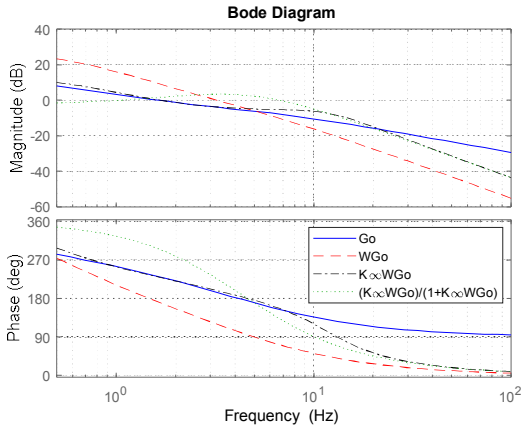

(a) Bode plots for robust loop-shaping design.

(b) Motor control system with the pre-compensator.

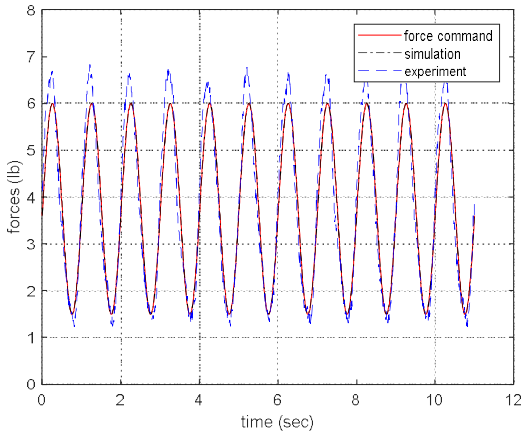

(c) Force tracking results.

Fig. 7 Control design for the motor control system.

V. NDT Rehabilitation Tests

We invited two stroke patients to undergo NDT training. The subjects took the Mini-Mental State Examination (MMSE) [25] and scored scores of more than 24, confirming their suitability for NDT training. They have signed informed consent forms approved by Human Subject Research Ethics Committee of IRB before participating.

We recorded the gait data using the VZ 4000 to analyze the effectiveness of rehabilitation. Because gait symmetry is a critical pattern for post-stroke walking rehabilitation, guiding the paralyzed side to shift the COG at the right time is the key point for initiating the stepping. Therefore, we select the following two performance indexes to evaluate the effectiveness of rehabilitation [26]:

1. Asymmetry of the swing phases: The swing phase of a leg is defined as the duration from the toe-off to the heel-strike of this leg. Therefore, the asymmetry of the swing phases during each gait can be defined as follows [26]:

$$Asym_{SP}(\%) = \frac{SP_{paretic} - SP_{non\text{-}paretic}}{SP_{paretic}} \times 100\% \qquad (12)$$

where $SP_{paretic}$ and $SP_{non\text{-}paretic}$ represent the swing time of the paretic and non-paretic limb, respectively. For example, $SP_{paretic}$ and $SP_{non\text{-}paretic}$ represent the swing time of the left and right limb, respectively, for patients with left side paretic

2. Asymmetry of the step length: The step length is defined as the distance between the heels when the fore heel strikes. Therefore, we can define the asymmetry of the step lengths during each gait as in the following [26]:

$$Asym_{SL}(\%) = \frac{SL_{paretic} - SL_{non\text{-}paretic}}{SL_{paretic}} \times 100\% \qquad (13)$$

where $SL_{paretic}$ and $SL_{non\text{-}paretic}$ represent the step length of the paretic and non-paretic limb, respectively. For instance, $SL_{paretic}$ and $SL_{non\text{-}paretic}$ represent the step lengths of the left and right limb, respectively, for patients with left side paretic.

NDT is expected to reduce the deviation in the swing time and step lengths of the two sides. Therefore, the treatment is thought effective when these asymmetry indexes approach zero. We will compare the effects of the NDT training by therapists and by the proposed trainer.

We invited the two test subjects to participate experiments by the following A-B-A procedures: before treatment (A), in treatment (B), and after treatment (A). The test subjects were guided by the therapists through the A-B-A procedure at intervals of about 3 min-6 min-3 min, respectively. The subjects then rested for about 30 mins before being guided by the automatic NDT trainer through the same A-B-A procedure with intervals of about 3 min-6 min-3 min, respectively. The asymmetry of the swing phases $Asym_{SP}$ and the asymmetry of the step length $Asym_{SL}$ of Patient I are shown in Fig. 8, where the improvement of asymmetry are notable. The statistical data of Fig. 8 is illustrated in Table II, where the subscripts $_{th}$ and $_{mot}$ indicate the procedures by therapists and the automatic NDT trainer, respectively. We calculate the average absolute values of the test subjects to evaluate the effectiveness in Table II, where the values in bold indicate improvement.

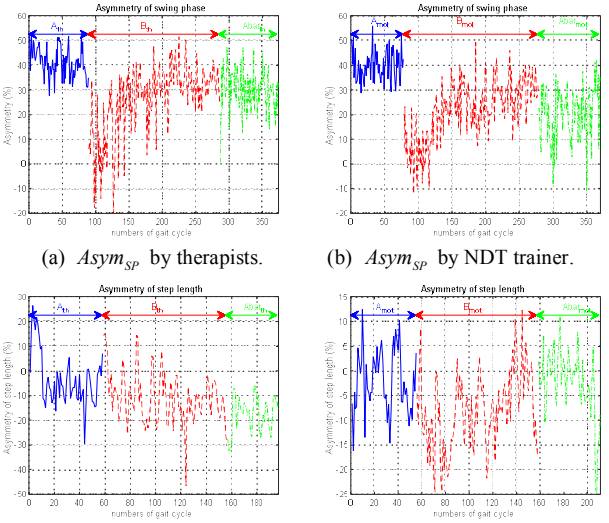

(a) $Asym_{SP}$ by therapists. (b) $Asym_{SP}$ by NDT trainer.

(c) $Asym_{SL}$ by therapists. (d) $Asym_{SL}$ by NDT trainer.

Fig. 8 Asymmetries responses of Patient I.

TABLE II. PERFORMANCE ANALYSES: AVERAGE AND STANDARD DEVIATION (IN PARENTHESIS)

Asymmetry of the swing phases $Asym_{SP}$ (%)						
	The therapist guiding			The NDT trainer guiding		
Subject	A_{th}	B_{th}	$\bar{A}_{th}$	A_{mot}	B_{mot}	$\bar{A}_{mot}$
Patient I	41 (6)	**26** (14)	**30** (8)	40 (6)	**22** (12)	**21** (11)
Patient II	6 (29)	**0** (**25**)	13 (30)	11 (28)	**-2** (27)	**3** (18)
Mean($\lvert\cdot\rvert$)	24 (8)	**13** (**20**)	**22** (19)	26 (9)	**12** (20)	**12** (15)
Asymmetry of the step lengths $Asym_{SL}$(%)						
	The therapist guiding			The NDT trainer guiding		
Subject	A_{th}	B_{th}	$\bar{A}_{th}$	A_{mot}	B_{mot}	$\bar{A}_{mot}$
Patient I	-25 (15)	**-13** (15)	**-8** (11)	-14 (12)	**-2** (11)	**-4** (13)
Patient II	-11 (10)	-16 (12)	**-8** (11)	-14 (12)	**-8** (14)	**-1** (11)
Mean($\lvert\cdot\rvert$)	18 (12)	20 (14)	**8** (11)	14 (12)	**5** (11)	**3** (10)

Reestablishment of gait symmetry in stroke patients is an important goal of rehabilitation. As indicated in Table II, the symmetries is in general improved during the treatment (B_{th} and B_{mot}), and the rehabilitation efficacies are sustained even after treatment ($\bar{A}_{th}$ and $\bar{A}_{mot}$). In addition, the improvements by the automatic NDT trainer are more significant than the therapist guidance. One possible reason is that the therapist guidance task was conducted first, so that practice effects were carried over to the next NDT trainer guidance task, i.e. the subjects gradually became familiar with the intervention by repeating practices.

The test results reveals positive training effects for short-term intervention. The designed automatic trainer can repeat the therapist's actions on the test subjects, so it can relieve the therapist's workload and increase the patient's training time. In addition, the treatment effectiveness can be sustained after the training. Because the NDT program is a long-term training process where the training effectiveness might be gradually improved, we plan to carry out long-term training tests in the future to evaluate the improvement.

VI. CONCLUSIONS

This paper has demonstrated the development and control design of an automatic NDT trainer. We first obtained clinical data from traditional NDT treatments and built an expert system to describe suitable intervention and patterns. Then, we constructed a motor control system and designed a robust loop-shaping controller to repeat therapist's actions. Last, we integrated the system and conducted experiments on stroke patients. We compared the rehabilitation results by two performance indexes. The results confirmed the effectiveness of the proposed automatic NDT trainer. The performance improvement by the trainer guidance was occasionally even better than the improvement by the therapist guidance, because the trainer provided objective judgments and did not become fatigued. We have conducted the tests in reverse order, i.e. by the trainer then by the therapist. The results also indicated the effectiveness of the designed trainer. In the future, we will recruit more test subjects and consider other performance indexes, such as the balance of COG and the symmetry of lateral pelvic displacement (LPD) [27, 28]. We also plan to conduct long-term training for more patients to confirm the effectiveness of the NDT trainer.

ACKNOWLEDGMENT

This work was financially supported in part by the Joint Project between Industrial Technology Research Institute of Taiwan and National Taiwan University and by the Ministry of Science and Technology, R.O.C. in Taiwan under Grands and MOST 106-2221-E-002-165-.

REFERENCES

[1] Ministry of Health and Welfare of ROC, Department of Statistics, "Ten leading causes of death", available at: http://www.mohw.gov.tw/CHT/DOS/Statistic.aspx?f_list_no=312&fod_list_no=5150

[2] M. J. Hall, S. Levant, C. J. DeFrances. (2012, May.). Hospitalization for stroke in US hospitals. *Diabetes*, *18(23)*, pp.1989–2009.

[3] A. S. Go, D. Mozaffarian, V. L. Roger, E. J. Benjamin, J. D. Berry, M. J. Blaha, et al. (2014). Heart disease and stroke statistics-2014 update. *Circulation*, *129(3)*.

[4] I. Díaz, J. J. Gil, E. Sánchez. (2011, Sep.). Lower-limb robotic rehabilitation: literature review and challenges. *Journal of Robotics 2011*.

[5] G. Colombo, M. Joerg, R. Schreier, V. Dietz. (2000, Dec.). Treadmill training of paraplegic patients using a robotic orthosis. *Journal of rehabilitation research and development*.

[6] H. Schmidt, C. Werner, R. Bernhardt, S. Hesse, J. Krüger. (2007, Feb.). Gait rehabilitation machines based on programmable footplates. *Journal of neuroengineering and rehabilitation*.

[7] J. Patton, D. A. Brown, M. Peshkin, J. J. Santos-Munné, A. Makhlin, E. Lewis, et al. (2008, May.). KineAssist: design and development of a robotic overground gait and balance therapy device. *Topics in stroke rehabilitation, 15(2)*, pp. 131-139.

[8] C. Schmitt, P. Métrailler. (2004, Sep.). The Motion Maker™: a rehabilitation system combining an orthosis with closed-loop electrical muscle stimulation. *In 8th Vienna International Workshop on Functional Electrical Stimulation*.

[9] https://infoscience.epfl.ch/record/81393/files/Paper_FESWS2004.pdf

[10] M. Pohl, J. Mehrholz, C. Ritschel, S. Rückriem. (2002, Feb.). Speed-dependent treadmill training in ambulatory hemiparetic stroke patients. *Stroke*, *33(2)*, 553-558.

[11] J. S. Vij, N. K. Multani. (2012, Jun.). Efficacy of neuro-developmental therapy based gait training in correction of gait pattern of post stroke hemiparetic patients. *Journal of Exercise Science and Physiotherapy*.

[12] E. Mikołajewska. (2013) The value of the NDT-Bobath method in post-stroke gait training. *Advances in Clinical and Experimental Medicine*.

[13] *VZ4000 tracker*, Phoenix Technologies Inc., available at: http://www.ptiphoenix.com/?prod-trackers-post=vz4000

[14] *EVa RT 4.0 User's Manual*. Santa Rosa, Motion Analysis Corporation, 2003.

[15] *DPM-3*, Transducer Techniques, available at: https://www.transducertechniques.com/load-cell-displays.aspx

[16] *NI myRIO-1900*, National Instrument, available at: http://sine.ni.com/nips/cds/view/p/lang/zht/nid/211694

[17] *Normal Gait Cycle*. EpoMedicine, available at: http://epomedicine.com/clinical-medicine/physical-examination-gait/

[18] *MPK-569-2.8A*, Hanmark Drive Technology Co., available at: http://hanmark.en.taiwantrade.com/

[19] A. Sano, L. Sun, H. Ohmori. (1999, Sep.). Direct closed-loop identification approach to unstable systems. In Control Conference (ECC) 1999 European.

[20] P. Van Overschee, B. De Moor. (1994, Jan.). N4SID: Subspace algorithms for the identification of combined deterministic-stochastic systems. *Automatica*, *30(1)*, pp. 75-93.

[21] K. Glover, D. McFarlane. (1989, Aug.). Robust stabilization of normalized coprime factor plant descriptions with H/sub infinity/-bounded uncertainty. *IEEE transactions on automatic control*, *34(8)*, pp. 821-830.

[22] T. T. Georgiou, M. C. Smith. (1990, Jun.). Optimal robustness in the gap metric. *IEEE Transactions on Automatic Control, 35(6)*, pp. 673-686.

[23] K. Zhou, J. C. Doyle, "Essentials of robust control," in Upper Saddle River, Vol. 104, NJ, Prentice hall, 1998.

[24] D. McFarlane, K. Glover. (1992, Jun.). A loop-shaping design procedure using H/sub infinity/synthesis. *IEEE transactions on automatic control*, *37(6)*, pp. 759-769.

[25] D. Mungas. (1991, Jul.). Iii-office mental status testing: A practical guide. *Geriatrics*. *46(7)*.

[26] G. Chen, C. Patten, D. H. Kothari, F. E. Zajac. (2005, Aug.). Gait differences between individuals with post-stroke hemiparesis and non-disabled controls at matched speeds. *Gait & posture, 22(1)*, pp. 51-56.

[27] K. J. Dodd, M. E. Morris. (2003, Aug.). Lateral pelvic displacement during gait: abnormalities after stroke and changes during the first month of rehabilitation. *Archives of physical medicine and rehabilitation*, *84(8)*, pp. 1200-1205.

[28] K. J. Dodd, M. E. Morris, T. A. Matyas, T. V. Wrigley, P. A. Goldie. (1998, May.). Lateral pelvic displacement during walking: retest reliability of a new method of measurement. *Gait & posture, 7(3)*, pp. 243-250.